Study on possible error in signal amplitude and time of arrival reconstruction

Dawid Pietruch

AGH University of Krakow, Faculty of Physics and Applied Computer Science

pietruch@agh.edu.pl

26.09.2024

This research was funded by the National Science Centre, Poland, under the grant no. 2021/43/B/ST2/01107

Motivation

This study was performed to understand possible errors in the reconstruction of amplitude and time of arrival using fit to raw data and deconvolution method.
Steps:

- Creating generator of virtual pulses which mimic raw data with given amplitude, TOA and level of noise
- Running deconvolution reconstruction on this data
- Comparison of methods which are responsible for choosing best set of samples for deconvolution
- Running fitting function for generated data

Two approaches to reconstruct amplitude of signal and time of arrival

Fitting of a theoretical CR-RC pulse

$$V(t) = \begin{cases} b, & \text{for } t < t_0. \\ \alpha \left(\frac{t-t_0}{\tau_{sh}}\right) e^{-\frac{t-t_0}{\tau_{sh}}} + b, & \text{for } t \geq t_0. \end{cases}$$

- pedestal subtraction
- pulse detection
- common mode subtraction
- signal amplitude and TOA reconstruction by applying fitting procedure

Deconvolution method

$$\mathrm{d}_i = v_i - 2e^{-\frac{T_{smp}}{\tau_{sh}}} v_{i-1} + e^{-\frac{2T_{smp}}{\tau_{sh}}} v_{i-2}$$

$$t_0 = \frac{\frac{d_2}{d_1} T_{smp}}{\frac{d_2}{d_1} + e^{-\frac{T_{smp}}{\tau_{sh}}}}$$

$$A = (d_1 + d_2) \left[\frac{\tau_{sh}}{T_{smp}} e^{\frac{T_{smp} - \tau_{sh}}{\tau_{sh}}} \right] \frac{e^{\frac{-t_0}{\tau_{sh}}}}{1 - \frac{t_0}{T_{smp}} \left(1 - e^{-\frac{T_{smp}}{\tau_{sh}}}\right)}$$

- pedestal subtraction
- pulse detection
- common mode subtraction
- calculating FIR samples (1 or 2 nonzero samples in ideal case)
- pair of FIR samples selection
- time of arrival calculation
- amplitude of signal calculation (based on selected FIR samples and calculated TOA)

Virtual pulse generator

Virtual pulse generator produce ideal CR-RC shaping pulses with additional Gaussian noise $n(\mu, \sigma)$, pulse start t_0, amplitude α and pedestal b

$$V(t) = \begin{cases} b + n(\mu, \sigma), & \text{for } t < t_0. \\ \alpha \left(\frac{t - t_0}{\tau_{sh}}\right) e^{-\frac{t - t_0}{\tau_{sh}}} + b + n(\mu, \sigma), & \text{for } t \geq t_0. \end{cases}$$

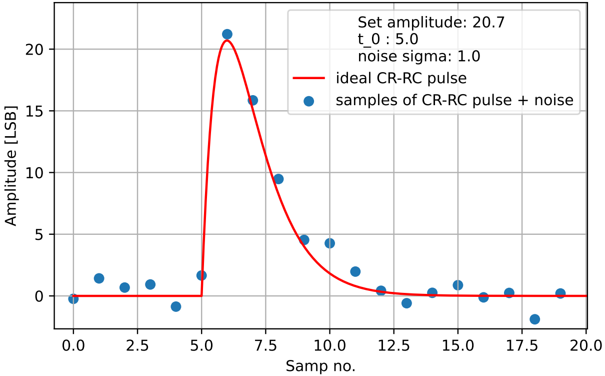

Fig. 1: An example of generated pulse and theoretical noiseless pulse

Animations

Fit performance - signal amplitude

Fitting function was checked on generated data without digitisation and additional noise σ=0 LSB.

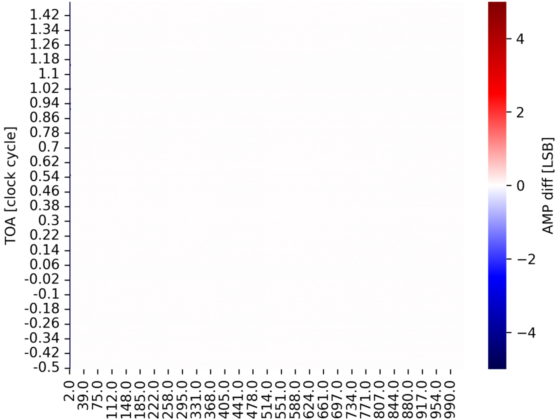

Fig. 2: Map of amplitude differences between set and reconstructed amplitude (reconstructed - set); fit reconstruction; noise σ=0 LSB

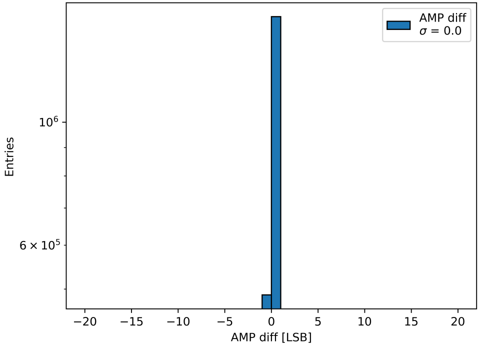

Fig. 3: Histogram of amplitude differences between set and reconstructed amplitude (reconstructed - set); fit reconstuction; noise σ=0 LSB

Fit performance - time of arrival

Fitting function was checked on generated data without digitisation and additional noise σ=0 LSB.

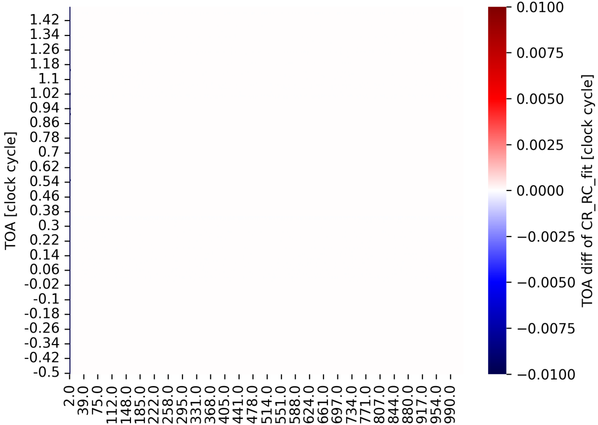

Fig. 4: Map of TOA differences between set and reconstructed TOA (reconstructed - set); fit reconstruction; noise σ=0 LSB

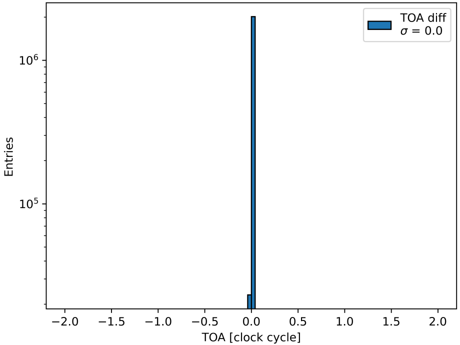

Fig. 5: Histogram of TOA differences between set and reconstructed TOA (reconstructed - set); fit reconstruction; noise σ=0 LSB

Digitisation error - signal amplitude

Influence of digitisation on amplitude reconstruction, noise σ=0 LSB.

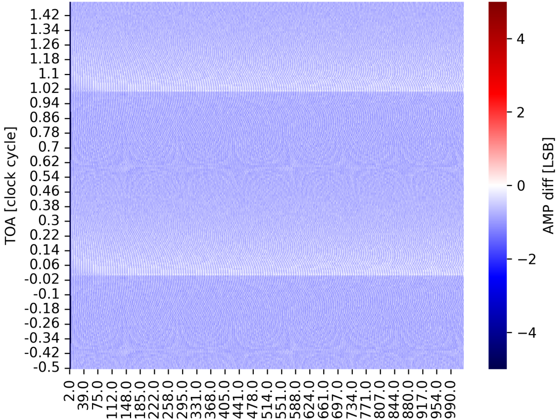

Fig. 6: Map of amplitude differences between set and reconstructed amplitude (reconstructed - set); fit reconstruction; noise σ=0 LSB

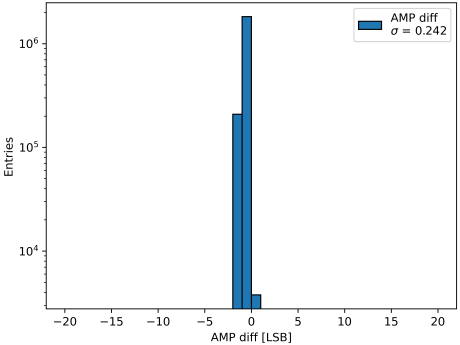

Fig. 7: Histogram of amplitude differences between set and reconstructed amplitude (reconstructed - set); fit reconstuction; noise σ=0 LSB

Digitisation error - signal amplitude

Influence of digitisation on amplitude reconstruction, noise σ=0 LSB.

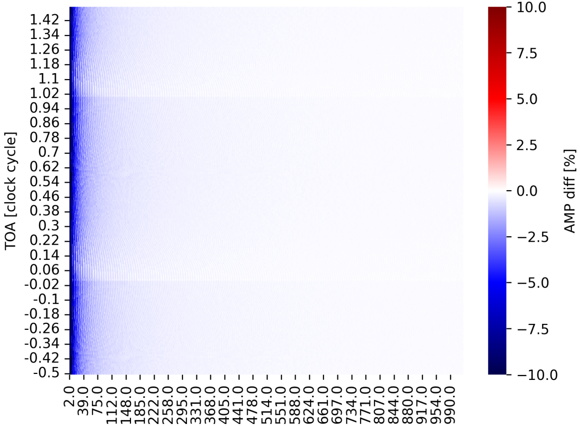

Fig. 8: Map of amplitude differences between set and reconstructed amplitude (reconstructed/set)-100%; fit reconstruction; noise σ=0 LSB

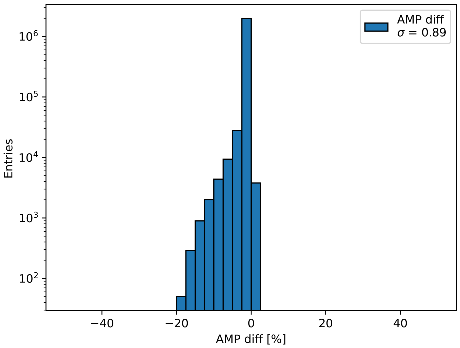

Fig. 9: Histogram of amplitude differences between set and reconstructed amplitude (reconstructed/set)-100%; fit reconstuction; noise σ=0 LSB

Digitisation error - time of arrival

Influence of digitisation on time of arrival reconstruction, noise σ=0 LSB.

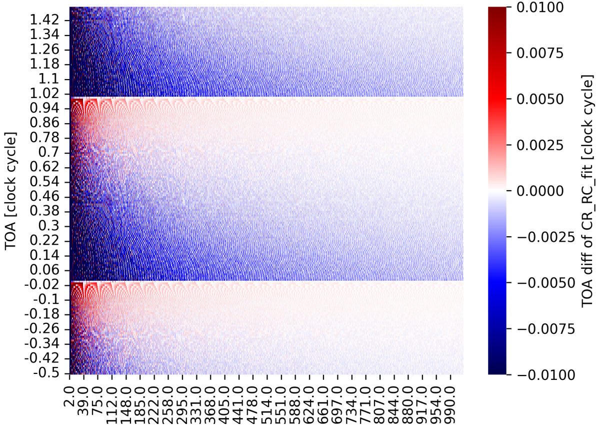

Fig. 10: Map of TOA differences between set and reconstructed TOA (reconstructed - set); fit reconstruction; noise σ=0 LSB

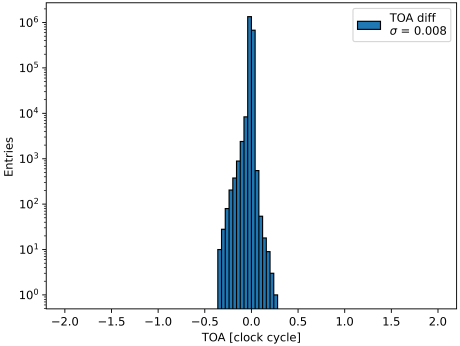

Fig. 11: Histogram of TOA differences between set and reconstructed TOA (reconstructed - set); fit reconstruction; noise σ=0 LSB

Noise influence - signal amplitude

To observe influence of noise on reconstruction of signal amplitude additional Gaussian noise were added to the samples; σ=1.0 LSB.

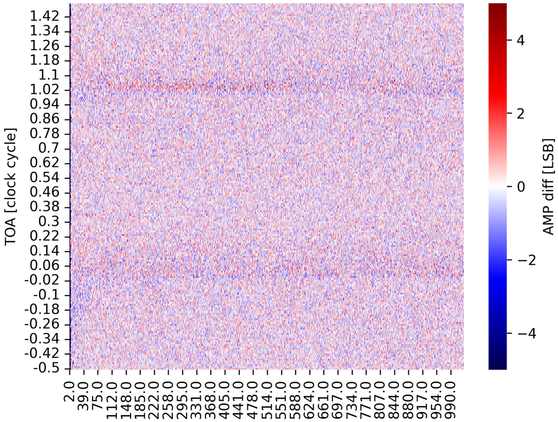

Fig. 12: Map of amplitude differences between set and reconstructed amplitude (reconstructed - set); fit reconstruction; noise σ=1.0 LSB

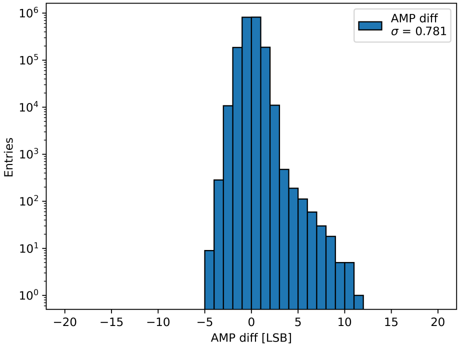

Fig. 13: Histogram of amplitude differences between set and reconstructed amplitude (reconstructed - set); fit reconstruction; noise σ=1.0 LSB

Noise influence - time of arrival

To observe influence of noise on reconstruction of TOA additional Gaussian noise were added to the samples; σ=1.0 LSB.

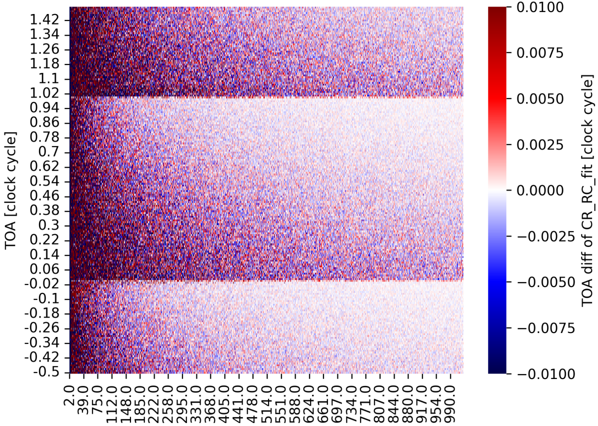

Fig. 14: Map of TOA differences between set and reconstructed TOA (reconstructed - set); fit reconstruction; noise σ=1.0 LSB

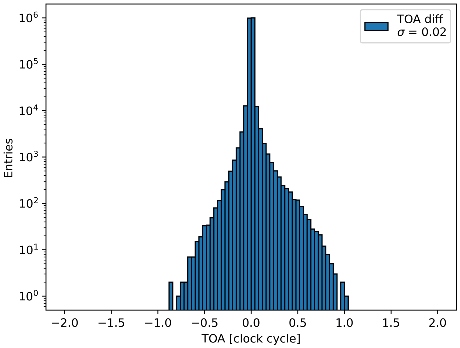

Fig. 15: Histogram of TOA differences between set and reconstructed TOA (reconstructed - set); fit reconstruction; noise σ=1.0 LSB

Noise and digitisation influence - signal amplitude

To observe influence of noise on reconstruction of signal amplitude additional Gaussian noise were added to the samples and digitisation was performed; σ=1.0 LSB.

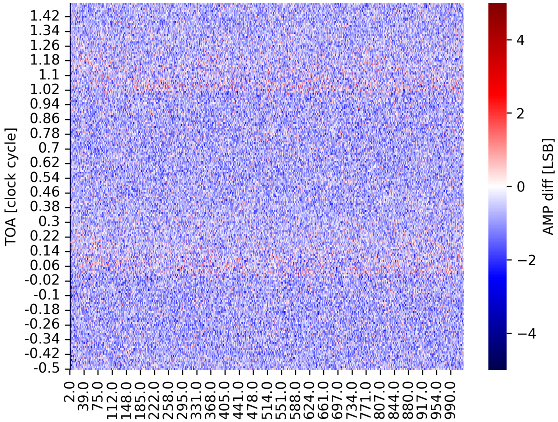

Fig. 16: Map of amplitude differences between set and reconstructed amplitude (reconstructed - set); fit reconstruction; noise σ=1 LSB

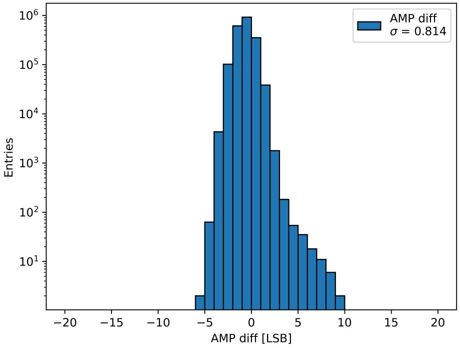

Fig. 17: Histogram of amplitude differences between set and reconstructed signal amplitude (reconstructed - set); fit reconstruction; noise σ=1.0 LSB

Noise and digitisation influence - signal amplitude

To observe influence of noise on reconstruction of signal amplitude additional Gaussian noise were added to the samples and digitisation was performed; σ=1.0 LSB.

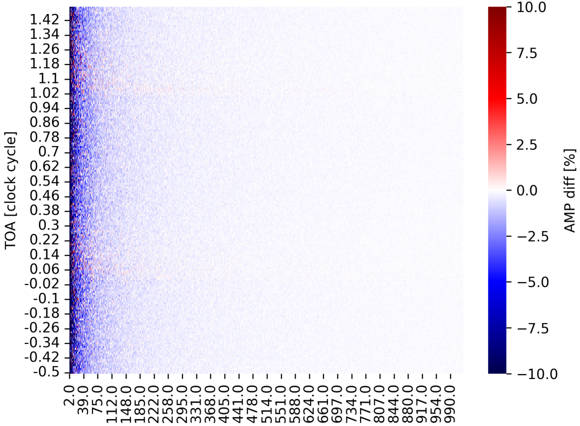

Fig. 18: Map of amplitude differences between set and reconstructed amplitude (reconstructed/set)-100%; fit reconstruction; noise σ=1.0 LSB

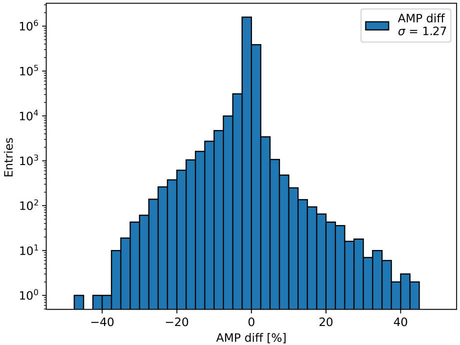

Fig. 19: Histogram of amplitude differences between set and reconstructed amplitude (reconstructed/set)-100%; fit reconstruction; noise σ=1.0 LSB

Noise and digitisation influence - time of arrival

To observe influence of noise on reconstruction of TOA additional Gaussian noise were added to the samplesand digitisation was performed; σ=1.0 LSB.

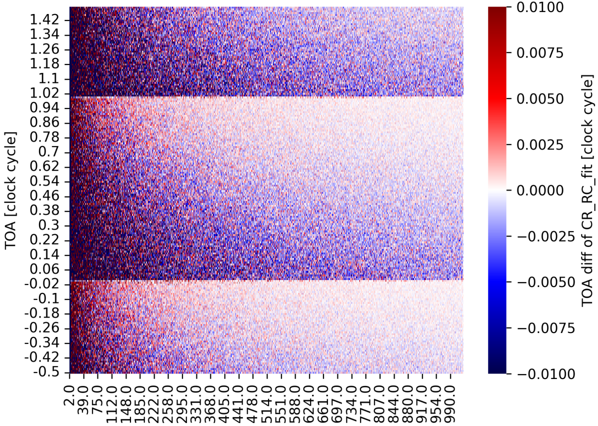

Fig. 20: Map of TOA differences between set and reconstructed TOA (reconstructed - set); fit reconstruction; noise σ=1.0 LSB

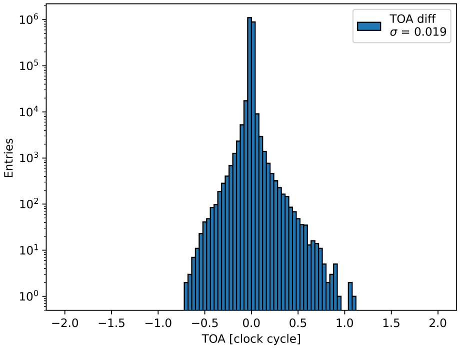

Fig. 21: Histogram of TOA differences between set and reconstructed TOA (reconstructed - set); fit reconstruction; noise σ=1.0 LSB

Which FIR samples should be used for deconvolution?

Different methods of determining the best pair of samples for deconvolution were checked.

First ADC sample above treshold

$\sigma = 1.089$ LSB

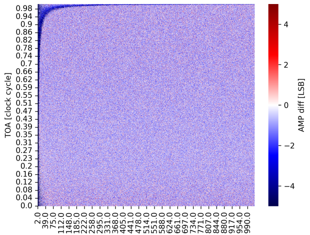

Fig. 22: Map of amplitude differences between set and reconstructed signal amplitude (reconstructed - set); fit reconstruction; noise σ=1.0 LSB

Max sample after FIR appling

$\sigma = 1.021$ LSB

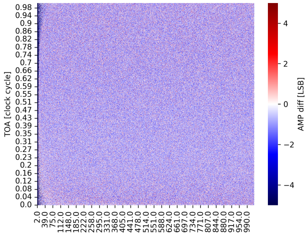

Fig. 23: Map of amplitude differences between set and reconstructed signal amplitude (reconstructed - set); fit reconstruction; noise σ=1.0 LSB

Max ADC sample

$\sigma = 1.019$ LSB

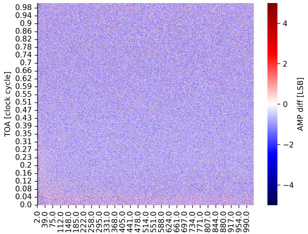

Fig. 24: Map of amplitude differences between set and reconstructed signal amplitude (reconstructed - set); fit reconstruction; noise σ=1.0 LSB

Which FIR samples should be used for deconvolution?

Different methods of determining the best pair of samples for deconvolution were checked.

First ADC sample above treshold

$\sigma = 1.089$ LSB

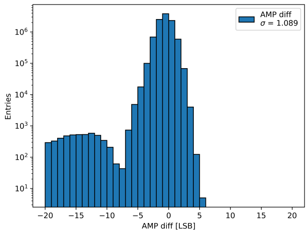

Fig. 25: Histogram of amplitude differences between set and reconstructed signal amplitude (reconstructed - set); deconvolution reconstruction; noise σ=1.0 LSB

Max sample after FIR appling

$\sigma = 1.021$ LSB

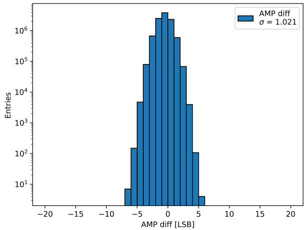

Fig. 26: Histogram of amplitude differences between set and reconstructed signal amplitude (reconstructed - set); deconvolution reconstruction; noise σ=1.0 LSB

Max ADC sample

$\sigma = 1.019$ LSB

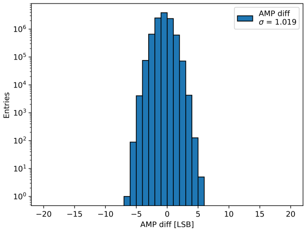

Fig. 27: Histogram of amplitude differences between set and reconstructed signal amplitude (reconstructed - set); deconvolution reconstruction; noise σ=1.0 LSB

Deconvolution digitisation influence - time of arrival

digitisation influence on deconvolution time o arrival reconstruction; ; σ=0.0 LSB.

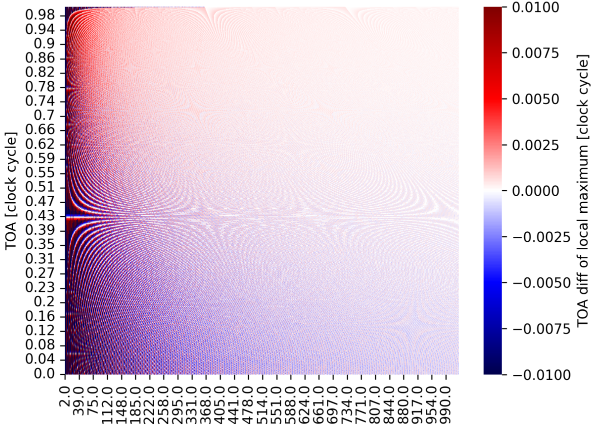

Fig. 28: Map of TOA differences between set and reconstructed TOA (reconstructed - set); deconvolution reconstruction; noise σ=0.0 LSB

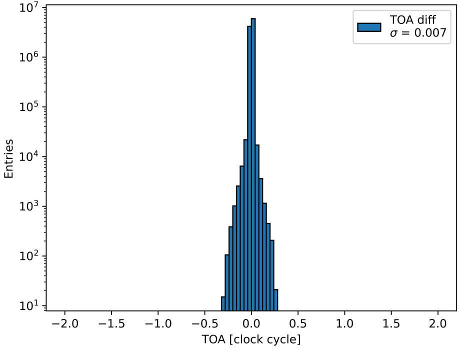

Fig. 29: Histogram of TOA differences between set and reconstructed TOA (reconstructed - set); deconvolution reconstruction; noise σ=0.0 LSB

Deconvolution digitisation influence - signal amplitude

digitisation influence on deconvolution amplitude reconstruction; σ=0.0 LSB.

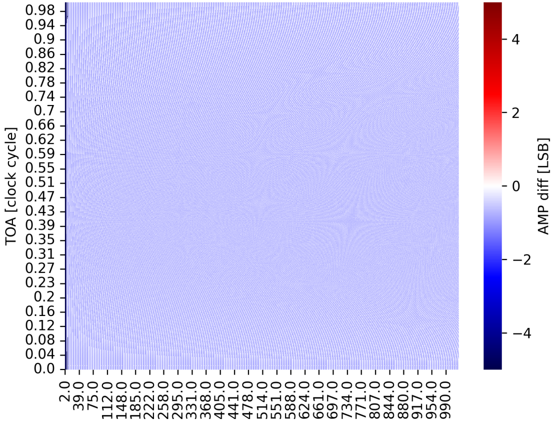

Fig. 30: Map of amplitude differences between set and reconstructed amplitude (reconstructed/set); deconvolution reconstruction; noise σ=0.0 LSB

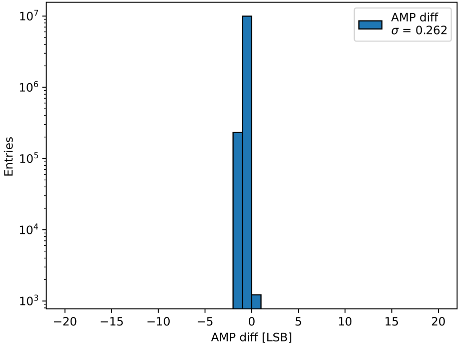

Fig. 31: Histogram of amplitude differences between set and reconstructed amplitude (reconstructed/set); deconvolution reconstruction; noise σ=0.0 LSB

Deconvolution digitisation influence - signal amplitude

digitisation influence on deconvolution amplitude reconstruction; ; σ=0.0 LSB.

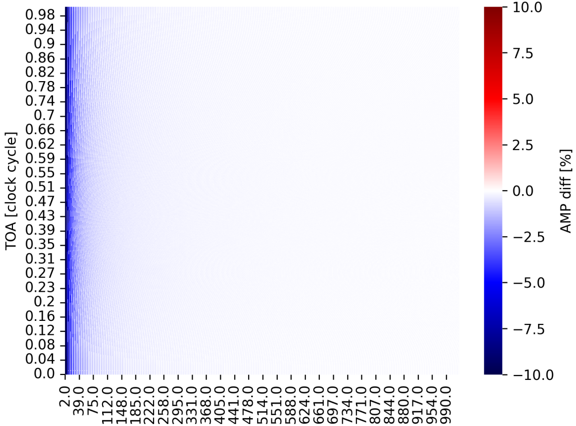

Fig. 32: Map of amplitude differences between set and reconstructed amplitude (reconstructed/set)-100%; deconvolution reconstruction; noise σ=0.0 LSB

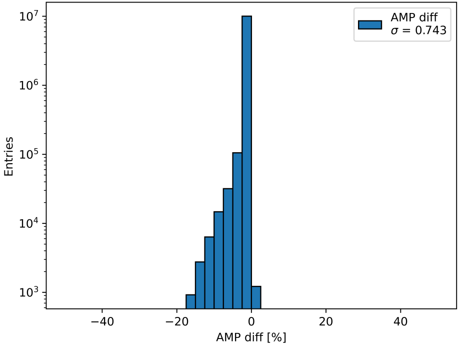

Fig. 33: Histogram of amplitude differences between set and reconstructed amplitude (reconstructed/set)-100%; deconvolution reconstruction; noise σ=0.0 LSB

Deconvolution noise and digitisation influence - time of arrival

To observe influence of noise on reconstruction of TOA additional Gaussian noise were added to the samples and digitisation was performed; σ=1.0 LSB.

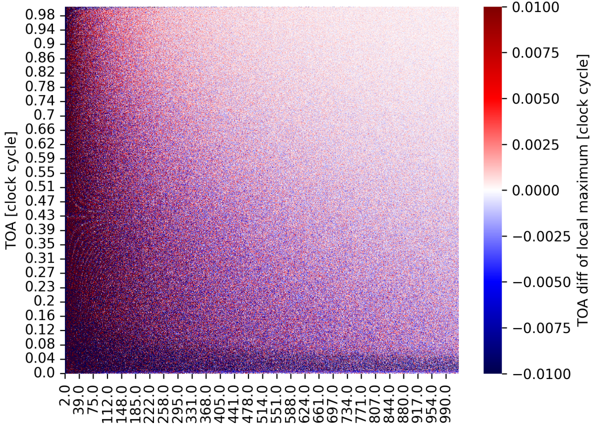

Fig. 34: Map of TOA differences between set and reconstructed TOA (reconstructed - set); deconvolution reconstruction; noise σ=1.0 LSB

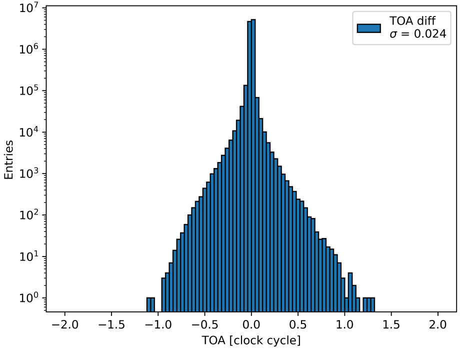

Fig. 35: Histogram of TOA differences between set and reconstructed TOA (reconstructed - set); deconvolution reconstruction; noise σ=1.0 LSB

Deconvolution noise and digitisation influence - signal amplitude

To observe influence of noise on reconstruction ofsignal amplitude additional Gaussian noise were added to the samples and digitisation was performed; σ=1.0 LSB.

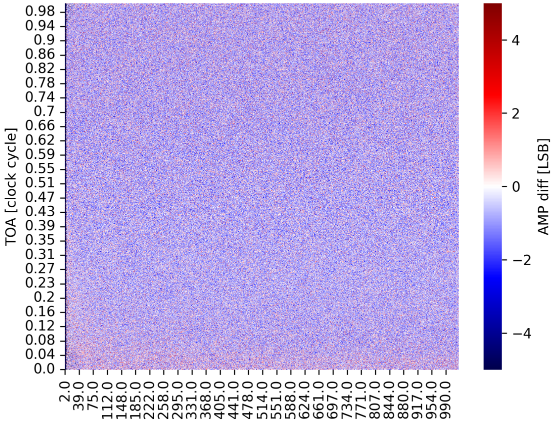

Fig. 36: Map of amplitude differences between set and reconstructed amplitude (reconstructed/set); deconvolution reconstruction; noise σ=1.0 LSB

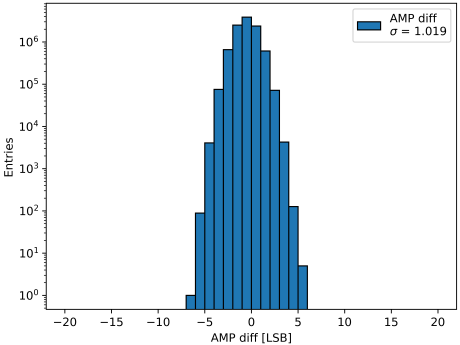

Fig. 37: Histogram of amplitude differences between set and reconstructed amplitude (reconstructed/set); deconvolution reconstruction; noise σ=1.0 LSB

Deconvolution noise and digitisation influence - signal amplitude

To observe influence of noise on reconstruction ofsignal amplitude additional Gaussian noise were added to the samples and digitisation was performed; σ=1.0 LSB.

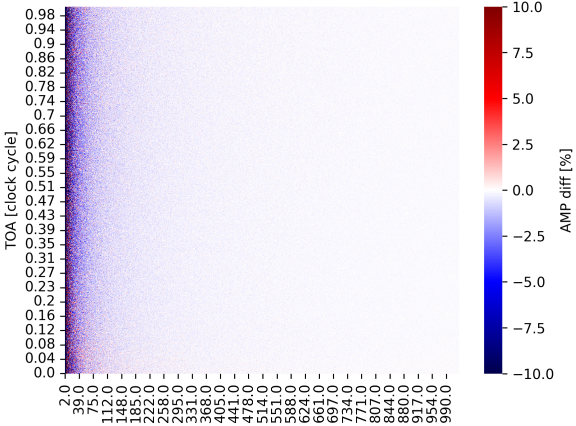

Fig. 38: Map of amplitude differences between set and reconstructed amplitude (reconstructed/set)-100%; deconvolution reconstruction; noise σ=1.0 LSB

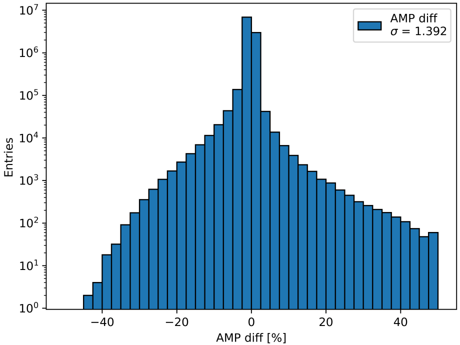

Fig. 39: Histogram of amplitude differences between set and reconstructed amplitude (reconstructed/set)-100%; deconvolution reconstruction; noise σ=1.0 LSB

Thank you for attention

Deconvolution method

Deconvolution method

In our front-end we uses CR-RC shaping, for which amplitude response over time can be written as formula below:

$$V(t) = \frac{q_{in}}{C_{feed}} \frac{t}{\tau_{sh}} e^{-\frac{t}{\tau_{sh}}} \tag{1}$$

If we include time before pulse, non-zero pulse start time t_0, amplitude α and pedestal b, equation 1 is transformed into:

$$V(t) = \begin{cases} b, & \text{for } t < t_0. \\ \alpha \left(\frac{t-t_0}{\tau_{sh}}\right) e^{-\frac{t-t_0}{\tau_{sh}}} + b, & \text{for } t \geq t_0. \end{cases} \tag{2}$$

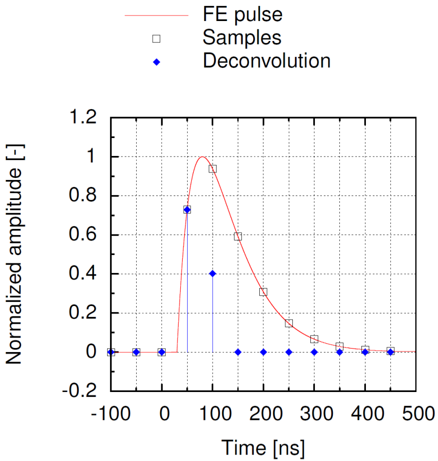

Fig. 40: Example of asynchronous sampling with two nonzero filter output samples at $t_0 = 30$ ns

Deconvolution method

Our output pulses are a convolution of its impulse response with the sensor's current signal (deposited charge), in order to find the input signal, we can use a procedure inverse to the convolution called deconvolution. In our system, this procedure is performed digitally by a digital filter. Output sample s_k of simplest FIR(Finite Impulse Response):

$$s_k = \sum_{i=0}^{N-1} w_i v_{k-i} \tag{3}$$

w_i - weight associated with input sample v_{k-i}

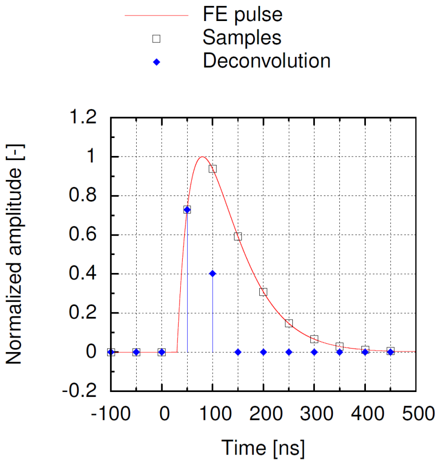

Fig. 41: Example of asynchronous sampling with two nonzero filter output samples at $t_0 = 30$ ns

Deconvolution method

To calculate amplitude of pulse we have to use some mathematical tools. Let start from front-end response $V_{sh}(s)$ in a Laplace domian can be expresed as:

$$V_{sh}(s) = \frac{1}{s} H(s) = \frac{1}{\tau_{sh}} \frac{1}{\left(s + \frac{1}{\tau_{sh}}\right)^2} \qquad (4)$$

$H(s)$ - transform function of the CR-RC shaper.

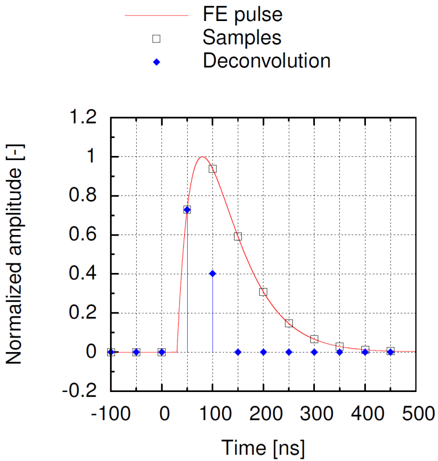

Fig. 42: Example of asynchronous sampling with two nonzero filter output samples at $t_0 = 30$ ns

Deconvolution method

Next step is to transform from continuous domain s to the discrete domain z using the Z transform. After that and we achieved discrete transform function $D(z)$:

$$D(z) = z^2 - 2e^{-\frac{T_{smp}}{\tau_{sh}}} z + e^{-\frac{2T_{smp}}{\tau_{sh}}} \quad (5)$$

Since z^2 represents the sample which will be received after 2 sampling periods, we can just multiplied by z^{-2} delaying all samples by two periods.

$$D(z) = 1 - 2e^{-\frac{T_{smp}}{\tau_{sh}}} z^{-1} + e^{-\frac{2T_{smp}}{\tau_{sh}}} z^{-2} \quad (6)$$

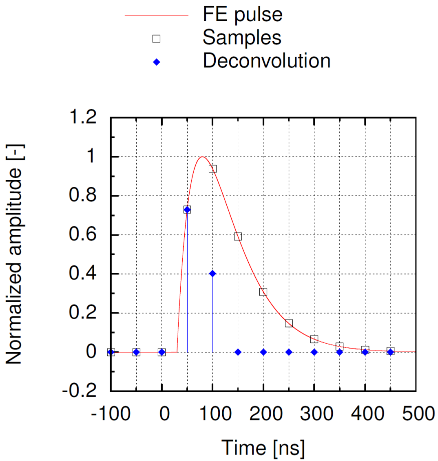

Fig. 43: Example of asynchronous sampling with two nonzero filter output samples at $t_0 = 30$ ns

Deconvolution method

Output sample value d_i, obtained at time $i \cdot T_{smp}$ can be expressed as:

$$d_i = v_i - 2e^{-\frac{T_{smp}}{\tau_{sh}}} v_{i-1} + e^{-\frac{2T_{smp}}{\tau_{sh}}} v_{i-2} \qquad (7)$$

where v_i is the shaper output:

$$v_i = V(i \cdot T_{smp}) \qquad (8)$$

If we calculate subsequent FIR output samples for CR-RC asynchronous shaper we can notice that filter produces only tow non zero samples or one in synchronous case.

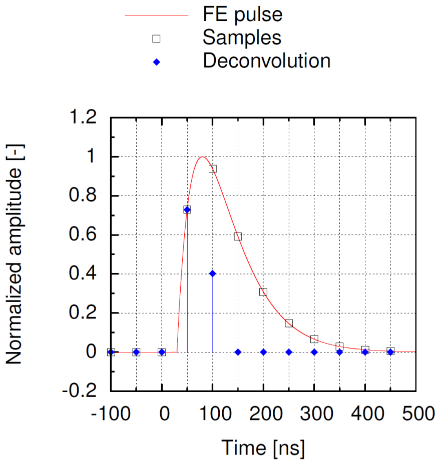

Fig. 44: Example of asynchronous sampling with two nonzero filter output samples at $t_0 = 30$ ns

Deconvolution method

Ratio between tow non-zero filter samples after reduction is given by:

$$\frac{d_2}{d_1} = \frac{t_0}{T_{smp} - t_0} e^{-\frac{T_{smp}}{\tau_{sh}}} \quad (9)$$

This ratio enable to calculate pulse starting time (TOA) which is necessary for amplitude reconstruction.

$$t_0 = \frac{\frac{d_2}{d_1} T_{smp}}{\frac{d_2}{d_1} + e^{-\frac{T_{smp}}{\tau_{sh}}}} \quad (10)$$

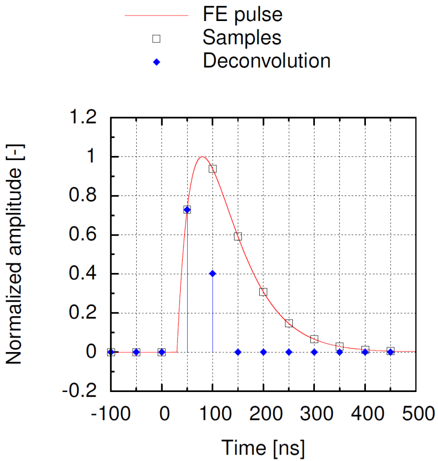

Fig. 45: Example of asynchronous sampling with two nonzero filter output samples at $t_0 = 30$ ns

Deconvolution method

Sum of two non-zero filter samples after reduction can be expressed as:

$$d_1 + d_2 = \frac{A}{\tau_{sh}} e^{-\frac{T_{smp} - t_0 - \tau_{sh}}{\tau_{sh}}} \left[T_{smp} - t_0 \left(1 - e^{-\frac{T_{smp}}{\tau_{sh}}} \right) \right] \quad (11)$$

This sum enable to calculate pulse amplitude A

$$A = (d_1 + d_2) \left[\frac{\tau_{sh}}{T_{smp}} e^{\frac{T_{smp} - \tau_{sh}}{\tau_{sh}}} \right] \frac{e^{\frac{-t_0}{\tau_{sh}}}}{1 - \frac{t_0}{T_{smp}} \left(1 - e^{-\frac{T_{smp}}{\tau_{sh}}} \right)} \quad (12)$$

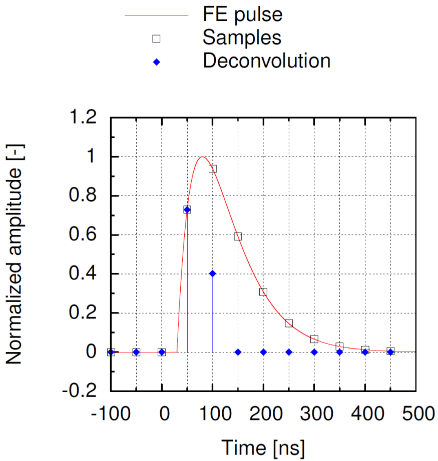

Fig. 46: Example of asynchronous sampling with two nonzero filter output samples at $t_0 = 30$ ns